4-5-2012

Genome-wide MicroRNA profiling of mantle cell lymphoma reveal a distinct subgroup with poor prognosis

Javeed Iqbal
University of Nebraska Medical Center, Omaha, NE

Yulei Shen
University of Nebraska Medical Center, Omaha, NE

Yanyan Liu
University of Nebraska Medical Center, Omaha, NE

Kai Fu
University of Nebraska Medical Center, Omaha, NE

Elaine Jaffe
Center for Cancer Research, NCI, NIH, Bethesda, MD

See next page for additional authors

Authors
Javeed Iqbal, Yulei Shen, Yanyan Liu, Kai Fu, Elaine Jaffe, Cuiling Liu, Zhongfeng Liu, Cynthia Lachel, Karen Deffenbacher, Timothy Greiner, Julie Vose, Sharathkumar Bhagavathi, Louis Staudt, Lisa Rimsza, Andreas Rosenwald, German Ott, Jan Delabie, Elias Campo, Rita Braziel, James Cook, Raymond Tubbs, Randy Gascoyne, James Armitage, Dennis Weisenburger, Timothy McKeithan, and Wing Chan

blood

Prepublished online April 5, 2012;
doi:10.1182/blood-2011-07-370122

Genome-wide MicroRNA profiling of mantle cell lymphoma reveal a distinct subgroup with poor prognosis

Javeed Iqbal, Yulei Shen, Yanyan Liu, Kai Fu, Elaine S. Jaffe, Cuiling Liu, Zhongfeng Liu, Cynthia M. Lachel, Karen Deffenbacher, Timothy C. Greiner, Julie M. Vose, Sharathkumar Bhagavathi, Louis M. Staudt, Lisa Rimsza, Andreas Rosenwald, German Ott, Jan Delabie, Elias Campo, Rita M. Braziel, James R. Cook, Raymond R. Tubbs, Randy D. Gascoyne, James O. Armitage, Dennis D. Weisenburger, Timothy W. McKeithan and Wing C. Chan

Blood (print ISSN 0006-4971, online ISSN 1528-0020), is published weekly by the American Society of Hematology, 2021 L St, NW, Suite 900, Washington DC 20036.

Blood First Edition Paper, prepublished online April 5, 2012; DOI 10.1182/blood-2011-07-370122

Genome-wide MicroRNA Profiling of Mantle Cell Lymphoma Reveal a Distinct Subgroup with Poor Prognosis

Javeed Iqbal[1]*, Yulei Shen[1]*, Yanyan Liu[1*, #], Kai Fu[1], Elaine S. Jaffe[2], Cuiling Liu[1], Zhongfeng Liu[1], Cynthia M. Lachel[1], Karen Deffenbacher[1], Timothy C. Greiner[1], Julie M. Vose[3], Sharathkumar Bhagavathi[1], Louis M. Staudt[4], Lisa Rimsza[5], Andreas Rosenwald[6], German Ott[7], Jan Delabie[8], Elias Campo[9], Rita M. Braziel[10], James R. Cook[11], Raymond R Tubbs[11], Randy D. Gascoyne[12], James O. Armitage[3], Dennis D. Weisenburger[1], Timothy W. McKeithan[3], and Wing C. Chan[1]

[1]Department of Pathology and Microbiology, University of Nebraska Medical Center, Omaha, NE, USA
[2]Laboratory of Pathology, Center for Cancer Research, NCI, NIH, Bethesda, MD, USA;
[3]Department of Hematology / Oncology, University of Nebraska Medical Center, Omaha, NE, USA;
[4]Metabolism Branch, Center for Cancer Research, NCI, NIH, Bethesda, MD, USA;
[5] Department of Pathology, University of Arizona, Tucson, Arizona, USA;
[6] Department of Pathology, University of Würzburg, Würzburg, Germany;
[7] Department of Clinical Pathology, Dr. Margarete Fischer-Bosch-Institute of Clinical Pharmacology, Robert-Bosch-Hospital, Stuttgart, Germany,
[8] Department of Pathology, The Norwegian Radium Hospital, University of Oslo, Oslo, Norway;
[9] Hospital Clinic, University of Barcelona, Barcelona, Spain.
[10] Clinical Pathology, Oregon Health, OR;
[11] Department of Molecular Pathology and Laboratory Medicine, Cleveland Clinic, Cleveland, OH;
[12]Center for Lymphoid Cancer, British Columbia Cancer Agency (BCCA), Vancouver, British Columbia, Canada
[#] Present address; Department of Internal Medicine, Institute of Lymphoma, Henan Cancer Hospital, Zhengzhou, China

Wing C. Chan. M. D.
Co-Director, Center for Research in Lymphoma and Leukemia
Department of Pathology and Microbiology
983135 Nebraska Medical Center
Omaha, NE 68198-3135
Phone: (402) 559-7684
Fax: (402) 559-6018
E-mail: jchan@unmc.edu

*Contribute equally

Running title: microRNA profiling in mantle cell lymphoma
Keywords: Mantle-cell lymphoma, Small lymphocytic leukemia, Molecular classifier, miRNA expression signature,

Presented in part, at the 51st American Society of Hematology (ASH) Annual Meeting, New Orleans, LA, December 5-8, 2009

Abstract

MicroRNA (miRNA) deregulation has been implicated in the pathogenesis of mantle cell lymphoma (MCL). Using a high-throughput quantitative real-time PCR platform, we performed miRNA profiling on cyclin D1-positive MCL (n=30) and cyclin D1-negative MCL (n=7) and compared them with small lymphocytic leukemia/lymphoma (SLL, n=12), aggressive B-cell lymphomas (n=138), normal B-cell subsets and stromal cells. We identified a 19-miRNA classifier which included six upregulated miRNAs (miR-135a, miR-708, miR-150, miR-363, miR-184, miR-342-5p) and 13 downregulated miRNAs, that was able to distinguish MCL from other aggressive lymphomas with >90% probability. Some of these upregulated miRNAs are highly expressed in naïve B-cells. MicroRNA classifier showed consistent results in FFPE tissues and was able to distinguish cyclin D1-negative MCL from other lymphomas. A 26-miRNA classifier could distinguish MCL from SLL, dominated by 23 upregulated miRNAs in MCL. Unsupervised hierarchical clustering of MCL cases demonstrated a cluster characterized by high expression of miRNAs from polycistronic miR17~92 cluster and its paralogs miR-106a-363 and miR-106b-25, which was distinct from the other clusters showing enrichment of stroma associated miRNAs. The corresponding gene-expression-profiling (GEP) data showed that the former cluster of MCL had significantly higher proliferation gene-signature (PS), while the other subsets had higher expression of stroma associated genes. Clinical outcome analysis suggests that miRNAs can serve as prognosticators.

Introduction

Mantle cell lymphoma (MCL) constitutes approximately 6% of all non-Hodgkin lymphomas and occurs predominantly in males of advanced age[1,2]. Several histological variants including the classical, small cell, blastoid and pleomorphic variants of MCL have been reported[1] with varying proliferation rates and genetic profiles[3,4]. The putative cell-of-origin is considered to be a naïve B-cell in the mantle zones or primary follicles. However, 20-30% of cases show mutated immunoglobulin variable-region heavy chain (IGHV) genes[2]. The immunophenotype is characterized by expression of B-cell associated antigens (CD20, CD22 and CD79), and CD5 with strong expression of IgM and IgD, but lack of CD23, CD10 and BCL6[1, 2]. Historically, the majority of MCL patients exhibited an aggressive clinical course, but this has improved with current management to a reported median survival of 5-7 years[5]. Recent studies have identified an indolent subtype of MCL with an even longer survival[6-7]. The neoplastic cells in these cases exhibit hypermutated *IGVH* genes, a non-complex karyotype and lack SOX11 expression.

The genetic hallmark of MCL is the t (11;14)(q13;q32), resulting in the overexpression of cyclin D1. Nonetheless, small subsets of cases (<5%) lack this genetic aberration, but exhibit an almost indistinguishable gene expression profile (GEP) and genomic profile compared to cyclin D1-positive cases[8, 9]. Several recurrent genetic abnormalities have been reported in MCL, including frequent losses of 9p21.3, 11q22-q23, and 22q11.22, and gains of 10p11.23 and 13q31.3[3, 4, 9]. Specific mutations and deletions in *p16 (CDKN2A), ATM, CHEK2* and *TP53* have also been frequently noted in MCL[2]. Partial uniparental disomy has also been reported in the regions that are frequently targeted by chromosomal deletions[10].

Abnormal miRNA expression has been implicated in the pathogenesis of lymphoma, including the recurrent 13q31.3 gain[9] harboring *MIHG1* which encodes the miR17~92 cluster composed of six polycistronic miRNAs (miR-17, miR-18a, miR-19a, mir19b-1, miR-20a and miR-92a). Alteration in miRNA expression has been explored in B-cell lymphomas including MCL[11-13]. We have performed a large scale global analysis on multiple types of B-cell lymphoma to compare with MCL, using a miRNA profiling platform based on high-throughput Taqman® quantitative real-time PCR (qRT-PCR). The study was aimed to identify

diagnostic and prognostic signatures in MCL, including cyclin D1-positive and -negative cases. The qRT-PCR assay permits highly accurate quantitation of individual miRNAs over a wide dynamic range and distinguishes between closely related miRNA family members. We also explored the applicability of this platform to both cryopreserved and formalin-fixed paraffin-embedded (FFPE) tissues. We correlated the miRNA profiles with the corresponding gene expression profiling (GEP) data as well to investigate the molecular mechanisms or pathways associated with deregulated miRNA expression.

Materials and methods

Patient samples, cell lines and normal primary cells

Frozen tumor specimens and fresh tonsils from routine tonsillectomy were obtained from patients with a protocol approved by the Institutional Review Board of University of Nebraska Medical Center. Tumor biopsies taken from a series of cyclin D1-positive MCL (n=30) and small lymphocytic lymphoma /chronic lymphocytic leukemia (SLL/CLL, n=12) patients were studied for miRNA and GEP. We compared these miRNA/GEP results to a series of diffuse large B-cell lymphoma (DLBCL) and Burkitt lymphoma (BL) (n=138). We compared miRNA profiles obtained from cryopreserved tissues with corresponding FFPE tissues in 8 (of 30) MCL, and 35 (of 138) DLBCL/BL samples. The other FFPE samples included cyclin D1-negative MCL (n=7), and GEP of 6 cases have been reported previously [8, 14]. A panel of expert hematopathologists reviewed and confirmed the diagnosis of cases using the World Health Organization classification[1]. The experimental details about cell lines and primary B-cells are included in supplemental Materials and method section.

The detailed protocol about (i) RNA isolation from fresh frozen and FFPE tissues for miRNA and/or gene expression profiling (ii) MicroRNA profiling and GEP data analysis (iii) immunological and fluorescence in-situ hybridization (FISH) analysis and (iv) Survival outcome analysis are included in supplemental Materials and method section.

Results

Patient characteristics

The clinical characteristics of the MCL and SLL patients are summarized in Table-1. The median age of the MCL patients (n=30) was 63 years (range 37-88 years) at the time of diagnosis with a high male to female ratio (5:1). These MCL patients exhibited an aggressive clinical course with a median OS of 2.98 years (Supplemental Figure-1). These cases were also profiled for gene expression and were classified as MCL with >90% confidence. Most of the cases were CD5+ and/or CD43+ and expressed cyclin D1 or showed cyclin D1 translocation by FISH (Supplemental Table-1a).

Of the other MCL cases (n=7) negative for t(11;14) and cyclin D1 expression, the GEP of six cases has been reported previously[8]. The seventh case, without GEP, showed MCL morphology and SOX11 expression consistent with other t(11;14) negative MCL cases. Similar to cyclin D1+ MCL cases, the median age at the time of diagnosis was 60 years (range 51-65) with male predominance (5 of 7 cases), and the cases also showed a similar immunophenotype, with expression of B-cell markers and CD5. The expression of SOX11 (7 of 7), and cyclinD2 (3 of 5) or D3 (2 of 5) was noted in the cyclin D1-negative cases (Supplemental Table-1b).

The median age of the SLL/CLL patients was 59 years (range 40-90) at the time of diagnosis with a male to female ratio of 2:1. These cases had the characteristic morphology and immunophenotype including lack of cyclin D1 expression. The majority (70%) of SLL/CLL patients had not received any chemotherapy, and the median follow-up since diagnosis was 6.2 years.

Molecular classifier for MCL based on miRNA profile

Unsupervised hierarchical clustering (HC) analysis revealed that the MCL and SLL cases formed a distinct cluster compared to other lymphoma entities (Figure-1A). Of the 30 MCL and 12 SLL/CLL cases, only one case each clustered separately in a DLBCL clusters. However, both cases were molecularly classified as

MCL or SLL with the miRNA classifiers upon further analysis (see paragraph below), indicating that the tumors still maintained a substantial differentiation-associated miRNA profile.

Further examination of the miRNA profile showed that two prominent miRNA signatures were differentially expressed among the major lymphoma entities: one signature reflected miRNAs highly expressed in stromal cells, and they were more highly expressed in DLBCL and BL. The other signature was associated with non-dividing, quiescent cells (naïve, resting PB), which was highly represented in MCL or SLL/CLL cases. These observations are consistent with the morphological findings that MCL lacks a major stromal component compared with DLBCL and that most MCL cases are not as proliferative as other aggressive lymphomas.

We used a Bayesian algorithm to derive a miRNA classifier that differentiate MCL from DLBCL/BL and LOOCV for classification precision[15]. This algorithm resulted in a 19-miRNA classifier, which included 6 upregulated miRNAs (miR-135a, miR-708, miR-150, miR-363, miR-184 and miR-342-5p) and 13 downregulated miRNAs (Figure-1B). When this signature was evaluated in normal B-cell subsets, the majority of the upregulated miRNAs were also highly expressed in either naïve B-cells, resting B-cells or CC, with the exception of miR-135a and miR-708, which were normally more highly expressed by CB/CC and stromal cells respectively. However, they were also expressed by two MCL cell lines JEKO and/or JVM2. The majority (8 of 13) of downregulated miRNAs (miR-424, miR-382, miR-376c, miR-127-3p, miR-539, miR-379, miR-376a, and miR-411) were expressed by stromal cells at a higher level, consistent with a low stromal content in MCL. The expression of the other downregulated miRNAs was also low in naïve B-cell and resting B-cells.

Morphological evaluation of the discrepant cases identified by miRNA classifier

We evaluated the precision of the miRNA classifier by LOOCV and observed that two cases of GEP defined DLBCL (n=89) were misclassified as MCL with >90% probability. These two cases were classified as ABC-DLBCL (n=1) and unclassifiable-DLBCL (n=1) by GEP analysis. However, upon morphological review,

these cases were compatible with the paraimmunoblastic variant of SLL. It was also noted that in general SLL/CLL cases had a high association (80-90% probability) with the MCL classifier and therefore, required a separate analysis (see below).

Only one MCL case showed probability <90 % by the miRNA classifier (see Figure 1B). This case was different from the other one that clustered within DLBCL cases in unsupervised HC (see Figure1A), but by miRNA classifier showed >95% probability as MCL. This case upon review showed blastoid-variant morphology.

Comparison of miRNA expression profile between MCL and SLL

As expected from the close clustering of MCL and SLL cases (Figure-1A), the miRNAs in the MCL classifier (derived from comparison with DLBCL/BL) showed significant overlap with the SLL cases with the exception of four miRNAs (miR-363, miR-184, miR-708 and miR-135a), which were highly expressed in MCL (Figure-1B). When only the MCL and SLL cases were analyzed by unsupervised HC, we observed two separate clusters (A and B) of SLL (Figure-2A). The SLL cluster-A showed mainly upregulated miRNAs compared with cases in cluster-B and was characterized by high expression of miRNAs shown to have tumor suppressive function (miR-1, miR-133a[16], miR-133b[16], miR-139-5p, miR-139-3p, miR-143[17], miR-10b[18] miR-145[16], miR23b) and stroma-related (miR-23a, miR-27a, miR-27b, miR-152, miR-221). One case each of two paraimmunoblastic SLL cases (*identified above*), clustered with SLL cluster-A and cluster-B, and showed no association with MCL clusters.

To more definitively separate MCL and SLL, we constructed a classifier consisting of 26 miRNAs that was dominated by 23 miRNAs upregulated in MCL, including miR-184 and members of two polycistronic miRNA clusters, miR106b-25 (miR-106b and miR-25) and miR106a-363 (miR-363 and miR-20b), which are paralogs of the miR17~92 cluster. In the classifier, only miR-150, miR-511 and miR-375 were significantly upregulated in SLL cases (Figure-2B). We observed that 5 MCL cases showed a probability of <90% [40-70% (4 case), 20% (1 cases)], and 1 case was classified as SLL suggesting that a small subset of

MCL cases may have a miRNA profile very similar to SLL cases. The latter two cases showed low expression of proliferation gene signature (PS) (log2 signal intensity 7.3, 7.6; range in 30 cases of PS is 6.9-9.1), and were part of the indolent MCL case cluster (see below). Interestingly the two SLL paraimmunoblastic variants, despite their much higher proliferation, showed significant similarity with the SLL group (80% and 90% probability respectively) in their miRNA expression profile (Figure-2B)

Identification of MCL subsets by miRNA profiling and correlation with GEP signatures

When MCL cases alone were analyzed by unsupervised HC, three distinct clusters were observed (Figure-3A) with a significant difference in expression of 95 miRNAs ($p<0.005$) among these clusters. We applied previously defined MCL proliferation gene expression signature (PS)[19], and observed a significant difference ($p=0.01$, Kruskal-Wallis Test) in the median expression of PS among the three miRNA-defined clusters, designated as cluster-A (high PS), cluster-B (medium PS) and cluster-C (low PS) (Figure-3A). The difference was more prominent between clusters-A and -C. The cases in cluster-A showed upregulation of miR17~92 cluster members and its paralogs miR-106a-363 and miR-106b-25, indicative of proliferative miRNA profile and a subgroup of miRNAs closely associated with CB, CC and cell lines, but not with naïve B-cell (Figure-3B)**.** The cases in cluster-C showed upregulation of miRNA having growth inhibitory functions including miR-1, miR-133b[16], miR-10b[18], and stroma-associated markers (miR-23a, miR-23b, let-7c, let-7-b, miR-125b). Of the differentially expressed miRNAs, miRNAs associated with stroma were significantly enriched in cluster-C, thus indicating the contribution of stroma in this subset of cases. The cluster-B cases showed low expression of majority of the miRNAs compared with clusters-A and -C, though high expression of miRNAs associated with stroma (miR-636, miR-539 and miR-485-3p) was noted specifically in this subset.

To further understand the biological significance of these clusters, we also examined the GEP data. Interestingly GEP–based unsupervised HC showed that cases in -cluster-A as defined by miRNA profile were almost identical to one of the three sub-clusters defined by GEP (all 8 cases in cluster-A) supporting

that cluster-A has distinctive molecular characteristics. When gene expression of the three miRNA-defined clusters was analyzed, 649 transcripts showed significant differential expression ($p<0.005$). Functional analysis showed that transcripts encoding proteins with roles in cell cycle progression and proliferation, or inhibition of apoptosis, were highly upregulated in cluster-A, consistent with the association with a high PS (Figure-3C). The transcript level of the proliferation marker *Ki67* was significantly associated with this group ($p<0.0001$). Additionally, in this group, we observed high expression of genes encoding proteins secreted by macrophages (e.g. *CHI3L1*) including *CD163* expressed in M2 macrophages. The cases in cluster-C (low PS group) compared to cluster-A (high PS group showed relatively high expression of genes encoding cytokines mainly associated with T-cells (*CX3CL1*, *CXCL12*, *CXCL2*, and *CXCL5*) and genes associated with WNT signaling (*FZD*, *WNT5A*, and *SFRP2*). The cases in this group also expressed transcripts encoding extracellular-matrix related proteins (*ECM2, EDN1, EGFR, EPS8, ITGA9* and *PDGFD*). Interestingly, many upregulated and downregulated genes in cluster-C showed similar expression pattern in cluster-B, however unique gene signature were also noted in these groups, but functional characteristics of these genes is limited in literature (Figure 3C). GSEA complemented above results, with significant enrichment of the proliferation-related gene signatures in cluster-A, whereas both of the other clusters showed enrichment of IL-6, TGF-β, hypoxia, VEFG, Hox10-induced and quiescent/stem cell-like gene signatures. Compared to cluster-C, cluster-B had a higher TGF-β signature and showed more genotoxic stress with higher p21 and ATM signatures, whereas cluster-C showed higher expression of WNT and IL-4 signaling pathway genes (Supplemental Table-2). We performed IHC of β-catenin on 3 representative cases from Cluster-C, and 2 cases from cluster-A. We observed strongly positive expression of β-catenin in stromal/endothelial cells in all 3 cases from Cluster-C. The vast majority of tumor cells are negative, whereas cases with high proliferation signature (cluster-A) show only occasional cell weakly positive for beta-catenin (Supplemental Figure 3) indicating that WNT activation may be attributed mostly to stromal components in Cluster-C cases.

Validation of GEP signatures: To further validate the GEP findings of these 30 MCL cases, we performed validation of the genes signatures in another cohort of MCL cases (n=82). In our initial analysis we derived a specific gene expression signature from the GEP data of the 30 MCL in this report (training data) that can distinguish Cluster-A and Cluster-C cases using Bayesian algorithm. This resulted in a 71 probe set with two gene signatures, one enriched in proliferation related genes (Signature-1) and the other enriched in stroma-related genes including WNT pathway genes (Signature-2) as indicated in supplemental Figure 4A. The mean expression level of these two gene signatures was inversely correlated and the ratio of the mean expression of the two signatures was significantly associated with EFS ($p<0.01$). We then analyzed the gene signatures in the independent MCL series (n=82) using hierarchical clustering, and obtained four subset of MCL cases with the majority of cases showing inverse correlation between Signature -1 and -2 expression. However, a small subset of cases expressed both signatures at similar levels (both high and both low). There is significant association of OS with the Signature-1 being predicting worse prognosis. When the ratio of expression of the two signatures was correlated with OS, higher ratios (Signature-1 vs 2) were associated with poorer prognosis (Supplemental Figure 4B).

Comparison of the naïve B-cells and MCL miRNA profile and functional implications

We identified a miRNA signature significantly associated with naive B-cells by comparison with other B-cell subsets, including CCs and CBs (supplemental Figure-2). The miRNAs significantly associated with naïve B-cell subsets were miR-150, miR-223, miR-342-3p, miR-146-5p, miR-95, miR-342-5p, and miR-146b-3p, with at least 4 of the 7 miRNAs noted in previous studies[20-22]. These upregulated miRNAs were also observed in resting B- and T- cells and showed marginal enrichment in MCL cases compared to other lymphoid entities(data note shown), but were largely absent from lymphoid cell lines.

To identify miRNAs that may have pathogenetic significance, we compared the miRNA profile of normal naïve B-cells to that of MCL. Excluding differences that may be attributable to the stromal elements, we observed that the majority (>80%) of differentially expressed miRNAs were upregulated in MCL compared

to naïve B-cells (Figure-4). The miRNAs upregulated in MCL but not in naïve B-cells or in stromal elements included miR-184, miR-21, miR-10b and miR-135a, whose oncogenic roles have been demonstrated in several malignancies[23-26], but the functional characteristics of many other upregulated miRNAs is not known. Only a few miRNAs were downregulated in MCL compared with normal naïve B-cells; however, these included some of the most abundant miRNAs (miR-150, miR-223, miR-222, and miR342-5p/3p) in naïve B-cells, suggesting that low expression of these miRNAs may be important for the pathogenesis of MCL (Figure 4).

Evaluation of cryopreserved and FFPE miRNA profile

The miRNA classifier obtained from cryopreserved tissues was evaluated in corresponding FFPE MCL (n=8) and DLBCL/ BL (n=35) cases. Of the 19 miRNAs, 2 miRNAs showed inconsistent expression in the FFPE cases; but remaining 17 miRNAs were able to distinguish MCLs from DLBCLs and BLs with similar sensitivity and specificity. The expression pattern of this 17-miRNA signature was similar between cyclin D1-positive and cyclin D1-negative MCL cases (n=7) and they were clearly classified, when compared with DLBCL/BL cases (Figure-5A).

Cyclin D1-negative vs -positive MCL: Despite the substantial similarity in miRNAs profiles, cyclin D1-positive and -negative MCL cases clustered separately in unsupervised HC, and showed 30 differentially expressed miRNAs ($p<0.05$ and 4-fold differences) (Figure-5B,C). The differences included down-regulation of miRNAs negatively regulated by MYC (miR-15a, miR-22, miR-29a, miR-29b, miR-29c and miR-142-3p)[27] and upregulation of oncomiR miR-155[28] in cyclin D1-negative MCL cases. In contrast, cyclin D1-positive cases showed significant upregulation of miR-27 and miR-19a, thus suggesting distinct pathogenetic mechanisms in these two subgroups of MCL. In addition, we did not observe significant expression changes of miRNAs located on 11q13 (miR-1237, miR-192, miR-194-2, miR-612, miR-548, miR-139, and miR-326) encompassing the CCND1 locus between cyclin D1 positive and -negative MCL cases.

Association of miRNA profile with clinical outcome

The correlation of miRNA expression with clinical outcome was evaluated by (i) correlation with the mRNA based proliferation signature; and (iii) using the Bair *et al*[29] unsupervised principle to identify miRNAs, which predict OS or EFS with PS as a covariate in the analysis. When miRNAs were analyzed with respect to the mRNA-based PS, 28 miRNAs were significantly ($p<0.05$) differentially expressed between the highest-tertile (n=10) and lowest-tertile (n=10) proliferative subgroups (Figure-6A). The high proliferative group is characterized by high expression of miR-18a of the miR17~92 cluster and miR-18b, miR-20b, and miR-363 of the miR-106a-363 cluster, indicating a proliferative miRNA signature[30, 31]. The low proliferative group included miR-125-3p, miR-126, miR-10b, miR-143 and miR-145, many of which were highly expressed in stromal cells, suggesting that the lower proliferative group is associated with a higher microenvironment signature.

We also performed survival risk prediction and a multivariate proportional hazards model was developed using PS as one of the covariate. We identified a six-miRNA signature (high expression of miR129-3p, miR-135a, miR-146a, miR-424, miR-450-5p and low expression of miR-222), separating MCL into good (median OS, ~4 years) and poor prognostic groups (median OS, ~ 2 years) independent of miRNAs associated with PS (Figure-6C and Supplemental Table-3b).

Discussion

We profiled 187 cases of B-cell lymphoma and subsets of normal B-cells, with the goals of constructing a reliable miRNA classifier for MCL, identifying miRNA based predictors of outcome, and determining possible roles of miRNA in the pathogenesis of MCL. Since the putative cell of origin for MCL is naïve, pre-germinal center B-cell, we determined miRNAs associated with naïve B-cells and their expression pattern in other quiescent B-cells. These miRNAs included miR-150, miR-223, miR-29a, miR-29c, miR-101, miR-320, miR-331, let-7b, miR-26a, and miR-342, some of these (miR-150, miR-29c, miR-101, miR-223, miR-320) have been previously reported as enriched in naïve B-cells, using multiple platforms including deep

sequencing[21, 22]. Some of these miRNAs may have a role in maintaining the quiescent state or uncommitted status of B-cells in peripheral lymphoid organs. For example, the expression of miR-223 in naïve B-cells has been shown to block of the differentiation of naïve B-cells to GC B-cells by repressing LMO2 and MYBL1[21, 22]. Similarly, miR-150 controls B1 cell expansion and the humoral immune response in mice by targeting the key transcription factor MYB[32]. However, the miRNA profile of MCL showed substantial differences from that of naïve B-cells. Since the MCL contains stromal elements, we included the miRNA profiles of stromal cells and T-cells isolated from the tonsils to facilitate our interpretation of the data. Though some changes in miRNA profiles on culturing the stroma cells may occur, but many miRNAs are associated with tissue of origin and we anticipate that this set of miRNA would be maintained. Although the stromal cells we generated represent only a portion of the tumor microenvironment, the expression of this stromal miRNA signature is clearly correlated with the abundance of stroma in a tumor (Figure-1). After excluding stromal miRNAs, there were still many overexpressed miRNA compared with naïve B-cells, suggesting that they may play a role in MCL. Of these, miR-135a has been demonstrated as oncogenic role by downregulating adenomatous polyposis coli (APC) and activating the WNT pathway in colorectal cancer[25] , but in classic Hodgkin lymphoma, it is associated with better prognosis and targets JAK2, resulting in downregulation of Bcl-xl[33]. The miR-21 has been demonstrated as an oncomiR in a pre-B-cell lymphoma mouse model[24], its direct targets include several tumor suppressor genes (*PTEN, PDCD4, ANP32A*)[34]. Similarly, the other upregulated miRNAs (miR-10a and -10b) are oncomiRs that induce cell motility and invasiveness by suppressing HOXD10[23]. Interestingly, miR-10a was downregulated in cluster-C (miRNA clustering Figure-3A/B) of MCL, and the HOX10-induced genes were correspondingly enriched in the same group when assessed by GEP. Consequently, low expression of miR-10a was significantly associated with better survival in MCL by univariate analysis (p=0.03). On the other hand, a few highly upregulated miRNAs in naïve B-cells (*vs* MCL), such as miR-150, miR-223 and miR-342-5p were also down-regulated in activated PB B-cells, suggesting that they regulate B-cell activation and that their downregulation may be important in terminating quiescence.

Our analysis identified a robust MCL miRNA classifier, which included 6 up- and 13 down-regulated miRNAs. The classifier was able to separate MCL cases from other aggressive lymphomas accurately in 29 of 30 cases with >90% probability. Interestingly, the only two DLBCL cases were misclassified. Upon further morphological examination, these two cases were diagnosed as the paraimmunoblastic variant of CLL, and showed similarity to MCL and SLL in their miRNA expression profiles. It is interesting that these two highly proliferative cases still retain sufficient similarity to MCL and SLL to be included in this category rather than DLBCL/BL. The analysis of miRNA profiling performed on the corresponding FFPE tissues showed similar results, thus demonstrating that the classifier performed with striking accuracy in FFPE tissues.

Of the miRNAs in the classifier, we observed a 45-fold downregulation of miR-150 upon differentiation of naïve B-cells to CBs. These observations suggest that miR-150 is a stage-specific marker of naïve B-cells and may block the transition of naïve B-cells to CB by downregulating MYB[32]. The association of miR-184 with MCL may partly be attributed to its presence in 15q25.1, which is frequently gained or amplified (>20%) in MCL[9], and has been functionally associated with cell proliferation and tumorigenesis[26]. The other upregulated miRNAs in the classifier with known roles include miR-135a[33] and miR-363[31] that have been implicated in oncogenesis. However, the classifier contains highly selected miRNAs and the study of miRNAs in tumor biology is more appropriately performed in the context of differentially expressed genes compared with the normal counterpart and other B-cell lymphomas as discussed above. Since the function of miRNAs may be context dependent, their reported functions may need to be validated in the cell type of interest.

We have demonstrated that the miRNA classifier for cyclin D1-positive MCL was very similarly expressed in cyclin D1-negative cases in FFPE tissues, which were all classified as MCL by this classifier. There are, however, sufficient differences that these two groups of cases tend to form their own clusters, when analyzed as a group. Of the differentially expressed miRNAs, miR-155 was upregulated while 6 miRNAs downregulated by MYC, including tumor suppressor miR-15a, were downregulated in cyclin D1-negative

MCL cases. Cyclin D1-positive cases showed significant upregulation of miR-27, miR-101, miR-142-5p, miR-19a, miR-19b, and two stroma-associated miRNAs, miR-126 and miR-143, compared to their cyclin D1-negative counterpart, suggesting subtle distinction in their pathogenesis. However, different miRNAs may affect the same oncogenic pathways through different mechanisms as illustrated by miR-155 (upregulated in cyclin D1-negative cases) and miR-19 (upregulated in cyclin D1-positive group) that may both activate the PI3K pathway by suppressing SHIP1 and PTEN, respectively.

The SLL cases showed a miRNA expression pattern similar to that of MCL, probably partly due to their low proliferation, the non-GC B-cell origin of the neoplastic cells, and their low stromal content, although the majority of cases do form a separate cluster (Figure-1A). Most SLL cases can also be differentiated from MCL by a miRNA classifier, with miR-150 showing marked upregulation in SLL, whereas 23 of the 26 other miRNAs showed higher expression in MCL, including miRNAs associated with the proliferation signature (miR-106b-25, miR-20b), pro-survival signal (miR-181a) *via* Bim down-regulation[35], and 15q amplification (miR-184)[9]. Only one case of each was misclassified into the other category, the misclassified SLL case was an aggressive paraimmunoblastic variant, and the misclassified MCL case belongs to cluster-C, which included more indolent cases.

By unsupervised HC, the miRNA expression profile segregated the MCL cases into three clusters that appeared to have biologic and clinical differences. Cluster-A showed high expression of proliferation-related miRNAs including the miR17~92 cluster[30] and its paralogs miR-106a-363 and miR-106b-25, also consistent with higher expression of proliferation-related genes. Contrary to cluster-A, cluster-C showed higher expression of stroma-associated miRNAs, including miR-23a, miR-23b, let-7c, let-7-b, miR-125b and miRNAs with growth inhibitory functions including miR-1, miR-133b[16], miR-10b[18]. GEP analysis also showed low expression of proliferation related genes and interestingly showed high expression of transcripts encoding extracellular matrix-related proteins (*ECM2, EDN1, EGFR, EPS8, ITGA9* and *PDGFD*). Further examination of these gene signatures in another MCL cohort (n=82) generally validated these findings. Most of the cases showed an inverse correlation between the signature enriched in proliferation associated genes

vs stromal associated genes and high ratio of these two signatures are associated with poorer survival. This observation suggests that the stroma may have influence on tumor cell proliferation. The influence of the tumor microenvironment on the outcome of patients with follicular lymphoma has been clearly demonstrated[36]. Similarly, in diffuse large B-cell lymphoma, the "stromal-1 signature", which is related to extracellular-matrix deposition, mesenchymal and histiocytic cells, is associated with favorable outcome[37]. Recently, we have also demonstrated the contribution of the stromal signatures in the prognosis of patients with angioimmunoblastic T-cell lymphoma[38]. This study suggests that a group of stroma-associated miRNAs may define a more indolent group of cases and warrant further investigation.

These MCL subgroups also showed differences in the expression of distinct signaling pathways when the associated GEP data were examined. Cluster-C showed enrichment of pathways associated with "stemness/quiescence" such as WNT and TGF-β signaling, whereas cluster-B appeared to be associated with higher genotoxic stress (enriched ATM and p21 pathway genes). Because of the reported role of WNT signaling in chronic lymphocytic leukemia (CLL)[39] and there is a previous report on the nuclear staining of β-catenin in neoplastic cells in 52% of MCL cases[40], we further investigated the expression of β-catenin by IHC. In our cases β-catenin seems to be mostly localized in stromal elements. Neither we nor our collaborators Elias Campo (personnel communication) were able to demonstrate nuclear expression of β-catenin in neoplastic MCL cells suggesting that WNT activation may be attributed mostly to stromal components in cluster-C cases. The effects of WNT signaling on B-cells are complex with studies indicating that WNT signaling is important in the proliferation of pro- and pre-B-cells[41]. WNT signaling has also been reported to be pro-survival in GC-B cells and in CLL cells but several studies have reported that activation of canonical WNT signaling in stromal cells inhibits B-cell lymphopoeisis[42] and WNT5a can signal through non-canonical WNT/Ca^{++} pathways to negatively regulate B-cell proliferation[43]. A more recent study has shown that activation of canonical WNT signaling in stromal cells blocked the proliferation and production of B and NK cells, as well as plasmacytoid dendritic cells[44], and induced expression of extracellular matrix genes. Since WNT signaling is observed in the least proliferative subset of MCL and β-catenin appears to be

in stromal cells, the possible role of microenvironmental miRNA in generating inhibitory signals to neoplastic MCL-cells, is intriguing and warrants further experimental studies.

Among the miRNAs upregulated in the high PS group, miRNAs from miR17~92 cluster and its two paralogs have been confirmed in promoting cell proliferation and inhibiting apoptosis[30]. We have also shown that miR17~92 targets PHLPP2, an important negative regulator of the PI3K/AKT pathway, in addition to PTEN and BIM, and overexpression of miR17~92 leads to constitutive activation of PI3K/AKT pathway and also chemoresistance in MCL cell lines[30]. In previous reports, high expression of miR17-5p and miR-20b in MCL was associated with short OS[12, 13]. In contrast, low expression of miR-29, whose target gene includes *CDK6* was associated with poor prognosis[11]. We observed that miR17 ~ 92 clusters and its paralogs miRNA-363 and some of the other miRNAs did correlate with the PS (Figure-6A). We generated a 6-miRNA prognosticator for MCL, independent of the PS. Of the 6 miRNAs, miR-222 and miR-146a are expressed at relatively higher levels and shows higher fold-difference (>3 fold) in expression between the two prognostic groups. Of these miR-146a[27] is repressed and miR-222[45] is induced by MYC and these miRNAs showed expected correlation with MYC mRNA expression, suggesting that MYC may play a role in MCL prognosis consistent with previous findings[46], and this may be partly mediated though the control of miRNA expression. It is interesting to note that miR-222 which is coexpressed as a cluster with miR-221 targets tumor suppressor $p27^{Kip1}$ [47], and loss of miR-146a promotes tumorigenesis in mice[48]. Aside from miRNAs that are correlated with the PS, there seems to be other miRNAs that could serve as predictors of survival. However due to limited number of cases in the analysis, more cases, particularly from clinical trial setting, will be needed to validate and refine this miRNA prognosticator in MCL.

Acknowledgments

This work was supported in part by a NCI grant (5U01/CA114778).We would like to thank Martin Bast for coordinating the clinical data, the Lymphoma Research foundation (MCL consortium) for providing the MCL cell lines, JEKO and JVM2 including in this study through the Lymphoma Cell Bank Collection (ATCC, Manassas, VA)

Author Contributions

YS, JI: designed and performed the experiments, analyzed the data and wrote the manuscript.

YL, CL, ZL, CML, and KD assisted in the design and performed experiments.

EJ, KF, TCG, SKB, LR, AR, JD, EC, JRC, RDG, DDW[1], LMS and WCC provide materials and perform pathology review or contribute to gene expression profiling data.

JOA and JMV provided the clinical data and other support.

TWM and WCC designed and supervised the research and wrote the paper.

Conflict of interest Disclosure

The authors have declared that no competing interests exist.

Reference

1. Steven H Swerdlow, Elias Campo, Harris NL, et al. WHO Classification: Pathology and Genetics of tumors of Haematopoietic and Lymphoid Tissues. *WHO;4*. Lyon,France: IARC Press; 2008.
2. Perez-Galan P, Dreyling M, Wiestner A. Mantle cell lymphoma: biology, pathogenesis, and the molecular basis of treatment in the genomic era. *Blood.* Jan 6 2011;117(1):26-38.
3. Salaverria I, Zettl A, Bea S, et al. Specific Secondary Genetic Alterations in Mantle Cell Lymphoma Provide Prognostic Information Independent of the Gene Expression-Based Proliferation Signature. *J Clin Oncol.* Feb 12 2007;25(10):1216-22.
4. Bea S, Ribas M, Hernandez JM, et al. Increased number of chromosomal imbalances and high-level DNA amplifications in mantle cell lymphoma are associated with blastoid variants. *Blood.* Jun 15 1999;93(12):4365-4374.
5. Herrmann A, Hoster E, Zwingers T, et al. Improvement of overall survival in advanced stage mantle cell lymphoma. *J Clin Oncol.* Feb 1 2009;27(4):511-518.
6. Orchard J, Garand R, Davis Z, et al. A subset of t(11;14) lymphoma with mantle cell features displays mutated IgVH genes and includes patients with good prognosis, nonnodal disease. *Blood.* Jun 15 2003;101(12):4975-4981.
7. Fernandez V, Salamero O, Espinet B, et al. Genomic and gene expression profiling defines indolent forms of mantle cell lymphoma. *Cancer Res.* Feb 15 2010;70(4):1408-1418.
8. Fu K, Weisenburger DD, Greiner TC, et al. Cyclin D1-negative mantle cell lymphoma: a clinicopathologic study based on gene expression profiling. *Blood.* Dec 15 2005;106(13):4315-4321.
9. Hartmann EM, Campo E, Wright G, et al. Pathway discovery in mantle cell lymphoma by integrated analysis of high-resolution gene expression and copy number profiling. *Blood.* Aug 12;116(6):953-961.
10. Vater I, Wagner F, Kreuz M, et al. GeneChip analyses point to novel pathogenetic mechanisms in mantle cell lymphoma. *Br J Haematol.* Feb 2009;144(3):317-331.
11. Zhao JJ, Lin J, Lwin T, et al. microRNA expression profile and identification of miR-29 as a prognostic marker and pathogenetic factor by targeting CDK6 in mantle cell lymphoma. *Blood.* Apr 1 2010;115(13):2630-2639.
12. Navarro A, Bea S, Fernandez V, et al. MicroRNA expression, chromosomal alterations, and immunoglobulin variable heavy chain hypermutations in Mantle cell lymphomas. *Cancer Res.* Sep 1 2009;69(17):7071-7078.
13. Di Lisio L, Gomez-Lopez G, Sanchez-Beato M, et al. Mantle cell lymphoma: transcriptional regulation by microRNAs. *Leukemia.* Jul 2010;24(7):1335-1342.
14. Mozos A, Royo C, Hartmann E, et al. SOX11 expression is highly specific for mantle cell lymphoma and identifies the cyclin D1-negative subtype. *Haematologica.* Nov 2009;94(11):1555-1562.
15. Simon R, Peng A. BRB-ArrayTools User Guide, version 4.2.0-Beta_1. Biometric Research Branch, National Cancer Institute. . http://linus.nci.nih.gov/BRB-ArrayTools.html.
16. Kano M, Seki N, Kikkawa N, et al. miR-145, miR-133a and miR-133b: Tumor suppressive miRNAs target FSCN1 in esophageal squamous cell carcinoma. *Int J Cancer.* Mar 2.
17. Noguchi S, Mori T, Hoshino Y, et al. MicroRNA-143 functions as a tumor suppressor in human bladder cancer T24 cells. *Cancer Lett.* Aug 28 2011;307(2):211-220.
18. Gabriely G, Yi M, Narayan RS, et al. Human Glioma Growth Is Controlled by MicroRNA-10b. *Cancer Res.* May, 2011 15;71(10):3563-3572.
19. Rosenwald A, Wright G, Wiestner A, et al. The proliferation gene expression signature is a quantitative integrator of oncogenic events that predicts survival in mantle cell lymphoma. *Cancer Cell.* Feb 2003;3(2):185-197.
20. Tan LP, Wang M, Robertus JL, et al. miRNA profiling of B-cell subsets: specific miRNA profile for germinal center B cells with variation between centroblasts and centrocytes. *Lab Invest.* Jun 2009;89(6):708-716.

21. Malumbres R, Sarosiek KA, Cubedo E, et al. Differentiation stage-specific expression of microRNAs in B lymphocytes and diffuse large B-cell lymphomas. *Blood.* Apr 16 2009;113(16):3754-3764.
22. Zhang J, Jima DD, Jacobs C, et al. Patterns of microRNA expression characterize stages of human B-cell differentiation. *Blood.* May 7 2009;113(19):4586-4594.
23. Ma L, Teruya-Feldstein J, Weinberg RA. Tumour invasion and metastasis initiated by microRNA-10b in breast cancer. *Nature.* Oct 11 2007;449(7163):682-688.
24. Medina PP, Nolde M, Slack FJ. OncomiR addiction in an in vivo model of microRNA-21-induced pre-B-cell lymphoma. *Nature.* Sep 2 2010;467(7311):86-90.
25. Nagel R, le Sage C, Diosdado B, et al. Regulation of the adenomatous polyposis coli gene by the miR-135 family in colorectal cancer. *Cancer Res.* Jul 15 2008;68(14):5795-5802.
26. Liu C, Teng ZQ, Santistevan NJ, et al. Epigenetic regulation of miR-184 by MBD1 governs neural stem cell proliferation and differentiation. *Cell Stem Cell.* May 7 2010;6(5):433-444.
27. Chang TC, Yu D, Lee YS, et al. Widespread microRNA repression by Myc contributes to tumorigenesis. *Nat Genet.* Jan 2008;40(1):43-50.
28. Costinean S, Zanesi N, Pekarsky Y, et al. Pre-B cell proliferation and lymphoblastic leukemia/high-grade lymphoma in E(mu)-miR155 transgenic mice. *Proc Natl Acad Sci U S A.* May 2 2006;103(18):7024-7029.
29. Bair E, Tibshirani R. Semi-supervised methods to predict patient survival from gene expression data. *PLoS Biol.* Apr 2004;2(4):E108.
30. Rao E, Jiang C, Ji M, et al. The miRNA-17- 92 cluster mediates chemoresistance and enhances tumor growth in mantle cell lymphoma via PI3K/AKT pathway activation. *Leukemia.* Nov 25. 2011 (in print)
31. Landais S, Landry S, Legault P, Rassart E. Oncogenic Potential of the miR-106-363 Cluster and Its Implication in Human T-Cell Leukemia. *Cancer Research.* 2007;7(12):5699.
32. Xiao C, Calado DP, Galler G, et al. MiR-150 controls B cell differentiation by targeting the transcription factor c-Myb. *Cell.* Oct 5 2007;131(1):146-159.
33. Navarro A, Diaz T, Martinez A, et al. Regulation of JAK2 by miR-135a: prognostic impact in classic Hodgkin lymphoma. *Blood.* Oct 1 2009;114(14):2945-2951.
34. Asangani IA, Rasheed SA, Nikolova DA, et al. MicroRNA-21 (miR-21) post-transcriptionally downregulates tumor suppressor Pdcd4 and stimulates invasion, intravasation and metastasis in colorectal cancer. *Oncogene.* Apr 3 2008;27(15):2128-2136.
35. Lwin T, Lin J, Choi YS, et al. Follicular dendritic cell-dependent drug resistance of non-Hodgkin lymphoma involves cell adhesion-mediated Bim down-regulation through induction of microRNA-181a. *Blood.* Dec 9 2010;116(24):5228-5236.
36. Dave SS, Wright G, Tan B, et al. Prediction of survival in follicular lymphoma based on molecular features of tumor-infiltrating immune cells. *N Engl J Med.* Nov 18 2004;351(21):2159-2169.
37. Lenz G, Wright G, Dave SS, et al. Stromal gene signatures in large-B-cell lymphomas. *N Engl J Med.* Nov 27 2008;359(22):2313-2323.
38. Iqbal J, Weisenburger DD, Greiner TC, et al. Molecular signatures to improve diagnosis in peripheral T-cell lymphoma and prognostication in angioimmunoblastic T-cell lymphoma. *Blood.* Feb 4 2010;115(5):1026-1036.
39. Lu D, Zhao Y, Tawatao R, et al. Activation of the Wnt signaling pathway in chronic lymphocytic leukemia. *Proc Natl Acad Sci U S A.* Mar 2 2004;101(9):3118-3123.
40. Gelebart P, Anand M, Armanious H, et al. Constitutive activation of the Wnt canonical pathway in mantle cell lymphoma. *Blood.* Dec 15 2008;112(13):5171-5179.
41. Reya T, O'Riordan M, Okamura R, et al. Wnt signaling regulates B lymphocyte proliferation through a LEF-1 dependent mechanism. *Immunity.* Jul 2000;13(1):15-24.
42. Yamane T, Kunisada T, Tsukamoto H, et al. Wnt signaling regulates hemopoiesis through stromal cells. *J Immunol.* Jul 15 2001;167(2):765-772.
43. Liang H, Chen Q, Coles AH, et al. Wnt5a inhibits B cell proliferation and functions as a tumor suppressor in hematopoietic tissue. *Cancer Cell.* Nov 2003;4(5):349-360.

44. Ichii M, Frank MB, Iozzo RV, Kincade PW. The canonical Wnt pathway shapes niches supportive for hematopoietic stem/progenitor cells. *Blood.* Feb 16 2012;119(7):1683-92
45. Kim JW, Mori S, Nevins JR. Myc-induced microRNAs integrate Myc-mediated cell proliferation and cell fate. *Cancer Res.* Jun 15 2010;70(12):4820-4828.
46. Hartmann E, Fernandez V, Moreno V, et al. Five-gene model to predict survival in mantle-cell lymphoma using frozen or formalin-fixed, paraffin-embedded tissue. *J Clin Oncol.* Oct 20 2008;26(30):4966-4972.
47. Kedde M, van Kouwenhove M, Zwart W, Oude Vrielink JA, Elkon R, Agami R. A Pumilio-induced RNA structure switch in p27-3' UTR controls miR-221 and miR-222 accessibility. *Nat Cell Biol.* Oct 2010;12(10):1014-1020.
48. Boldin MP, Taganov KD, Rao DS, et al. miR-146a is a significant brake on autoimmunity, myeloproliferation, and cancer in mice. *J Exp Med.* Jun 6;208(6):1189-1201.

Table 1: Characteristics of MCL (cyclin D1+) and SLL patients included in the study**

Clinical features		MCL n=30	SLL n=12
Age	**Median (range)**	63 (37 – 88)	59 (40 – 90)
Gender	**Female**	5 (17%)	3 (27%)
	Male	25(83%)	8 (63%)
Performance score	**<70**	3 (10%)	0 (0%)
	>70	27 (90%)	11 (100%)
Stage	**I/II**	2 (6%)	2 (18%)
	III/IV	28 (94%)	9 (82%)
Serum LDH	**Normal**	21 (70%)	9 (82%)
	Elevated	9 (30%)	2 (11%)
Number of extranodal sites	**<2**	26 (87%)	10 (91%)
	>2	4(13%)	1 (9%)
Survival (median)	**OS**	3.0	-
	EFS	1.5	6.2

OS; overall survival, EFS, event-free survival

** The characteristics of 6 (of 7) cyclin D1-negative MCL cases have been described previously (Fu K, *et al*. 2005), the seventh case, without GEP, showed MCL morphology and SOX11 expression consistent with other t (11;14) negative MCL cases. One of 12 SLL cases lacked complete clinical data.

Figure legend

Figure-1: (A) Unsupervised Hierarchical clustering of lymphoma samples, normal cells and cell lines. MCL, SLL, DLBCL and BL formed largely distinct clusters. A stromal cell associated miRNA signature is more highly expressed in DLBCL and BL cases. There are also significant differences in the expression of miRNA associated with naïve B, resting B, CB and CC, with miRNA associated with naive and resting B-cells more highly represented in MCL or SLL cases. (B) A miRNA classifier, derived using Bayesian algorithm resulted in a 19-miRNA classifier (6 upregulated and 13 downregulated miRNAs), can separate most MCL from DLBCL and BL cases. The expression of this miRNA classifier is illustrated in SLL, normal cells and cell lines. Golden boxes highlight naïve B-cell and MCL cell lines.

Figure-2: (A) Unsupervised hierarchical clustering of MCL and SLL samples showed two separate clusters of SLL cases with each having unique miRNA profiles. (B) A 26-miRNA signature differentiates MCL from SLL, with 23 miRNAs including two polycistronic miRNA clusters, miR106b-25 (miR-106b and miR-25) and miR106a-363 (miR-363 and miR-20b) significantly upregulated in MCL compared to SLL.

Figure-3: (A) Unsupervised hierarchical clustering of MCL cases, showed three distinct MCL clusters with significant difference in the proliferation gene expression signature (PS) among the three groups ($p=0.01$, Kruskal-Wallis Test). PS included the same gene set as identified in reference 34. (B) Differential miRNA expression (95 miRNAs, $p<0.005$) among these clusters; designated as cluster-A (associated with high PS), cluster-B (medium PS) and cluster-C (low PS). (C) Differential gene expression (649 transcripts, $p<0.005$) among the three clusters with cluster A showing high expression of genes associated proliferation, whereas the other clusters showing higher expression of genes associated with stromal components.

Figure-4: Comparison of the MCL miRNA profile with other B-cell subsets, T-cells and stromal elements. >80% of differentially expressed ($p<0.005$) miRNAs were upregulated in MCL compared with naive B-cells.

Figure-5: (A) MCL classifier obtained from cryopreserved tissues showed similar predictive power in FFPE tissues and cyclin D1-negative MCL are classified as MCL. (B) Unsupervised clustering based on miRNA profiles showed distinct clusters of cyclinD1-negative and cyclin D1-positive MCL cases. (C) Differential expression of miRNA between cyclin D1-negative and positive MCL cases.

Figure-6: Correlation of miRNA expression with clinical outcomes: (A) Differential miRNA expression between cases in highest-tertile (n=10) and lowest-tertile (n=10) of proliferation signature ($p<0.05$). (B) Kaplan-Meier curves of miRNAs-636 and miR-424 showing significant ($p<0.05$) association with overall survival on univariate analysis. (C) Kaplan-Meier curves for risk groups using 6-miRNA signature obtained for survival risk prediction by Bair's et.al principle.

Figure 1

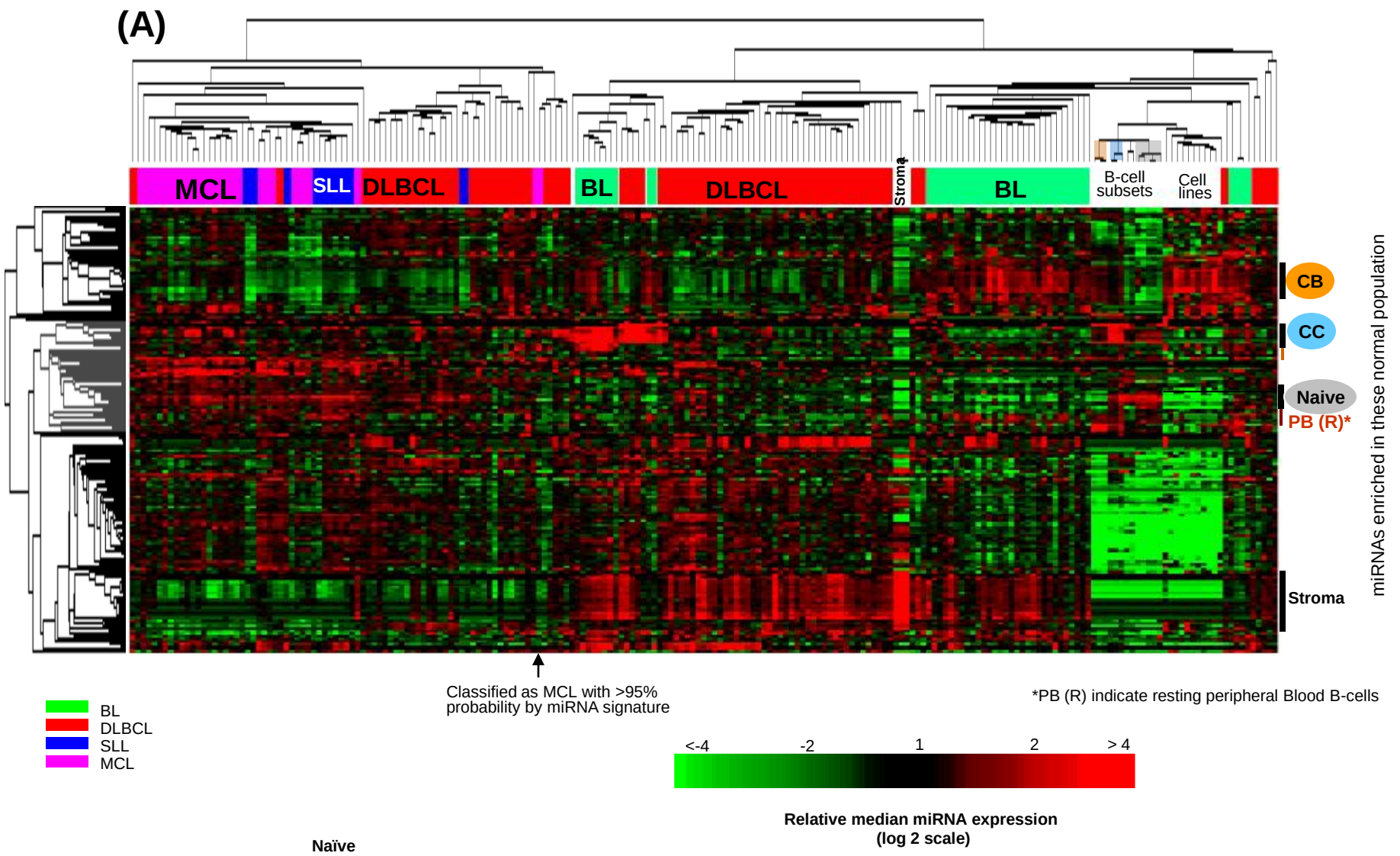
(A)
MCL
SLL
DLBCL
BL
DLBCL
Stroma
BL
B-cell subsets
Cell lines
CB
CC
Naive
PB (R)*
Stroma
miRNAs enriched in these normal population
Classified as MCL with >95% probability by miRNA signature
*PB (R) indicate resting peripheral Blood B-cells
BL
DLBCL
SLL
MCL
<-4
-2
1
2
> 4
Relative median miRNA expression
(log 2 scale)
Naïve

Figure 1

(B)

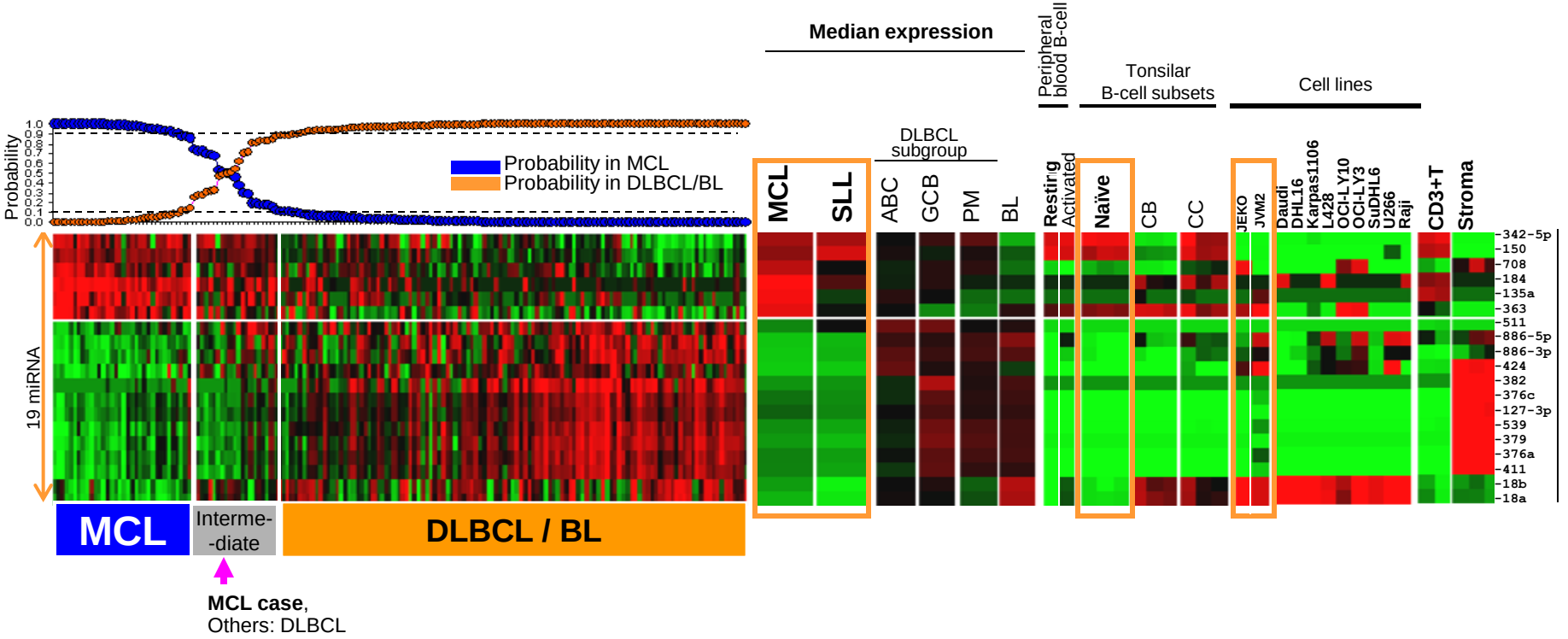
Median expression
Peripheral blood B-cell
Tonsilar B-cell subsets
Cell lines
DLBCL subgroup
Probability
Probability in MCL
Probability in DLBCL/BL
19 miRNA
MCL
SLL
ABC
GCB
PM
BL
Resting
Activated
Naïve
CB
CC
JEKO
JVM2
Daudi
DHL16
Karpas1106
L428
OCI-LY10
OCI-LY3
SuDHL6
U266
Raji
CD3+T
Stroma
342-5p
150
708
184
135a
363
511
886-5p
886-3p
424
382
376c
127-3p
539
379
376a
411
18b
18a
microRNA
MCL
Interme--diate
DLBCL / BL
MCL case,
Others: DLBCL

Figure 2

(A)

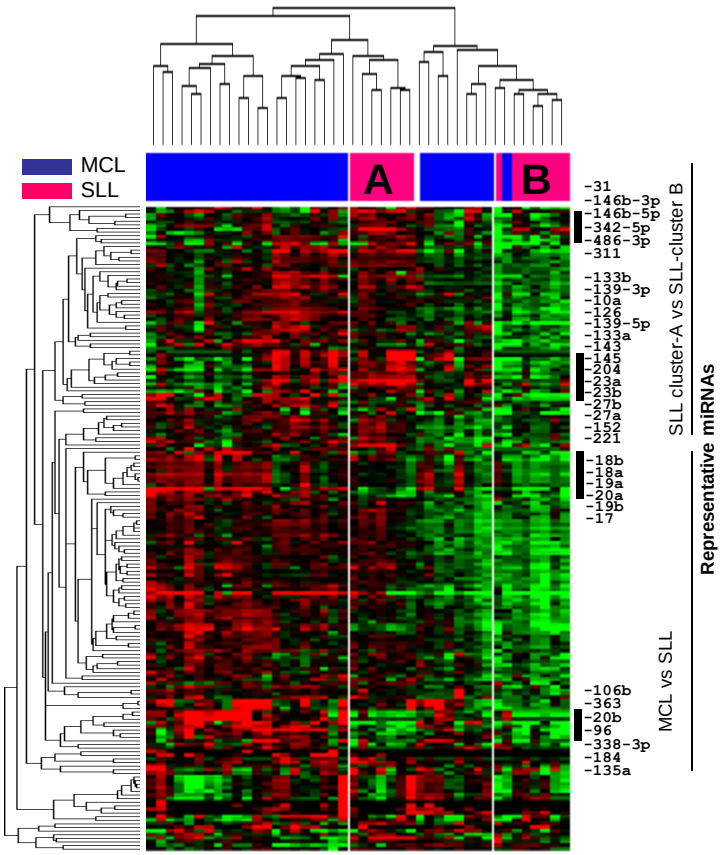
MCL
SLL
A
B
-31
-146b-3p
-146b-5p
-342-5p
-486-3p
-311
-133b
-139-3p
-10a
-126
-139-5p
-133a
-143
-145
-204
-23a
-23b
-27b
-27a
-152
-221
-18b
-18a
-19a
-20a
-19b
-17
-106b
-363
-20b
-96
-338-3p
-184
-135a
SLL cluster-A vs SLL-cluster B
MCL vs SLL
Representative miRNAs

(B)

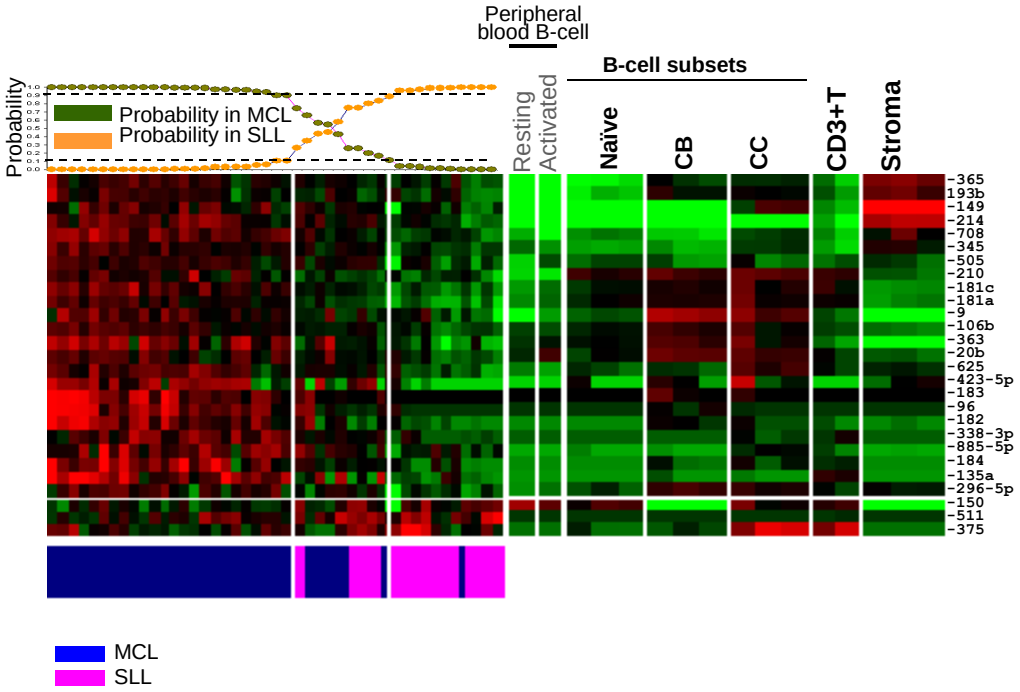
Peripheral blood B-cell
B-cell subsets
Probability
Probability in MCL
Probability in SLL
Resting
Activated
Naïve
CB
CC
CD3+T
Stroma
-365
193b
-149
-214
-708
-345
-505
-210
-181c
-181a
-9
-106b
-363
-20b
-625
-423-5p
-183
-96
-182
-338-3p
-885-5p
-184
-135a
-296-5p
-150
-511
-375
MCL
SLL

Figure 3

(A) miRNA- unsupervised hierarchical clustering

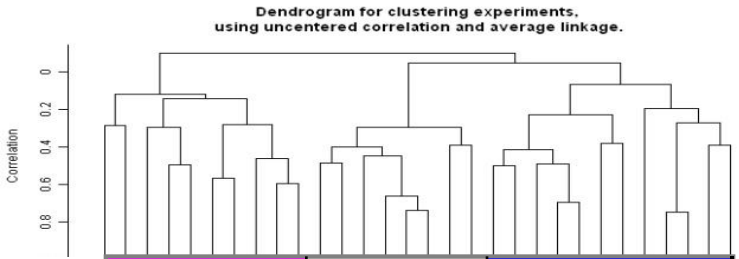

A	B	C
(n=10)	(n=8)	(n=12)
8.3 (7.5-9.1)	7.9 (7.3-8.3)	7.5 (6.9-8.1)

Proliferation index (median expression and range by GEP (log2 signal intensity)

(B) miRNA

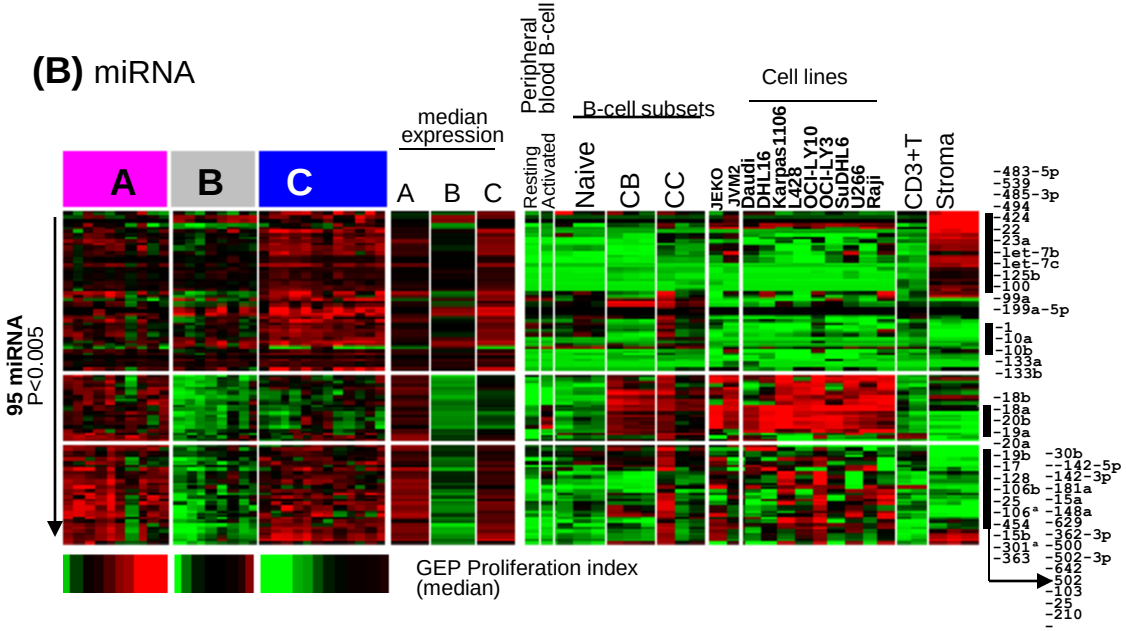

(C) mRNA

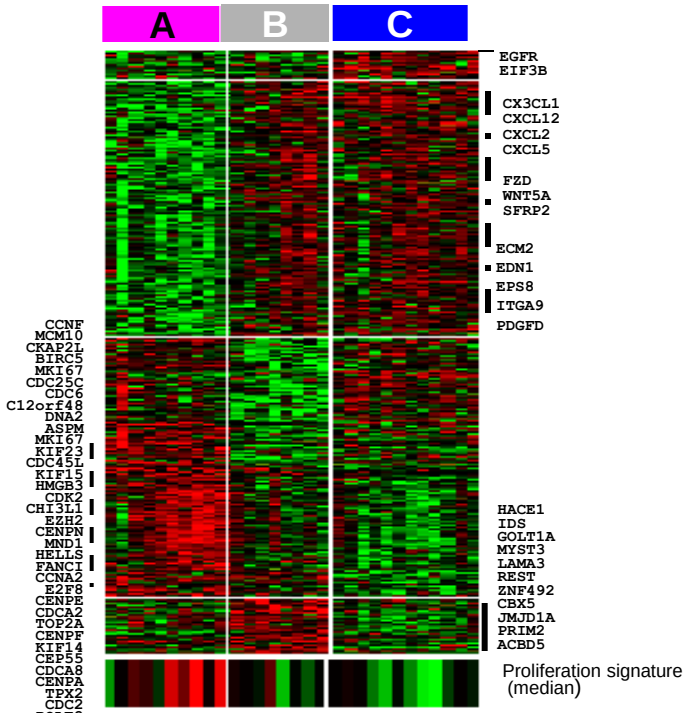

Figure 4

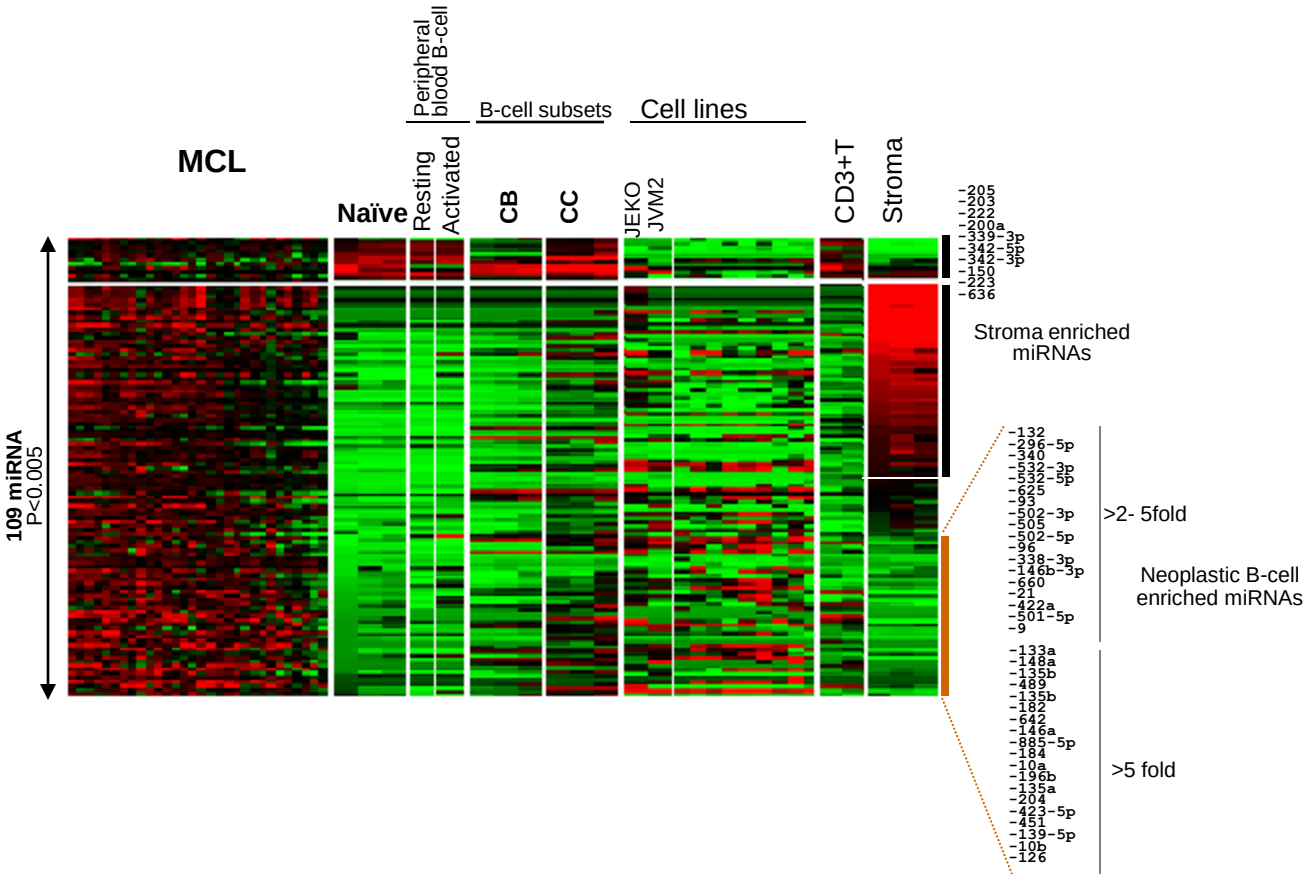
Peripheral blood B-cell
B-cell subsets
Cell lines
MCL
Naïve
Resting
Activated
CB
CC
JEKO
JVM2
CD3+T
Stroma
109 miRNA
P<0.005
-205
-203
-222
-200a
-339-3p
-342-5p
-342-3p
-150
-223
-636
Stroma enriched miRNAs
-132
-296-5p
-340
-532-3p
-532-5p
-625
-93
-502-3p
-505
-502-5p
-96
-338-3p
-146b-3p
-660
-21
-422a
-501-5p
-9
>2- 5fold
Neoplastic B-cell enriched miRNAs
-133a
-148a
-135b
-489
-135b
-182
-642
-146a
-885-5p
-184
-10a
-196b
-135a
-204
-423-5p
-451
-139-5p
-10b
-126
>5 fold

Figure 5

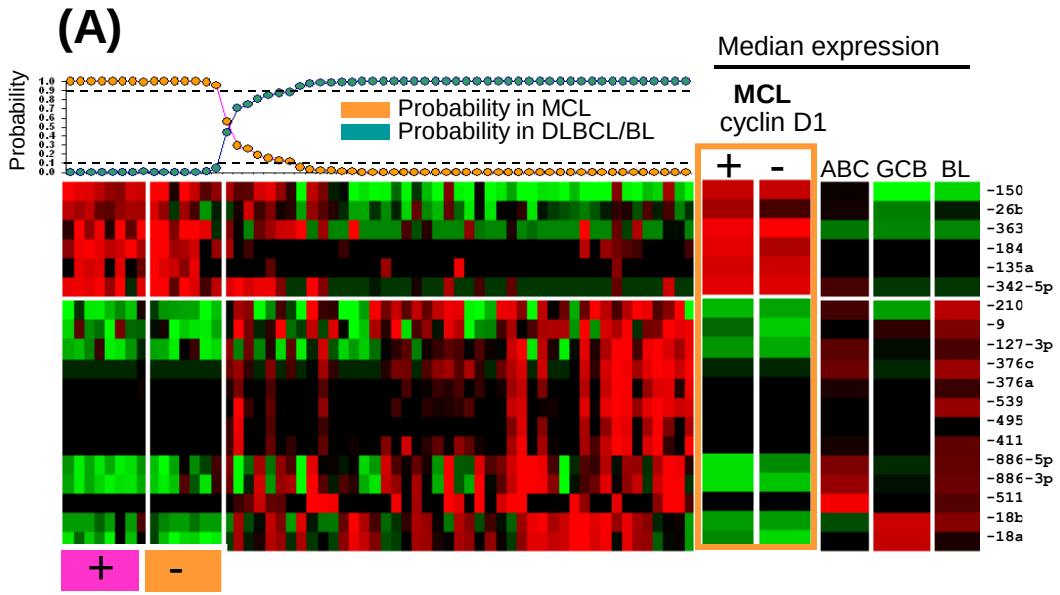
(A)
Median expression
MCL
cyclin D1
Probability
Probability in MCL
Probability in DLBCL/BL
+
-
ABC GCB BL
-150
-26b
-363
-184
-135a
-342-5p
-210
-9
-127-3p
-376c
-376a
-539
-495
-411
-886-5p
-886-3p
-511
-18b
-18a
+
-

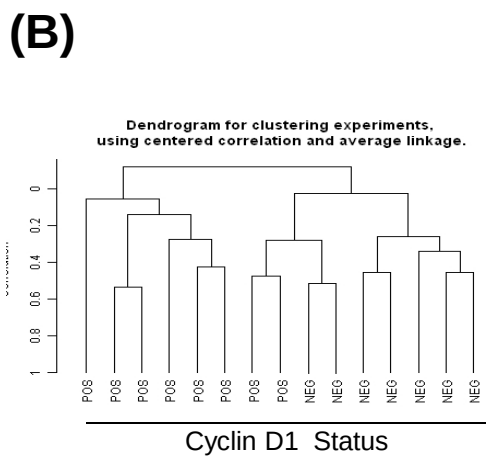
(B)
Dendrogram for clustering experiments,
using centered correlation and average linkage.
POS POS POS POS POS POS POS POS NEG NEG NEG NEG NEG NEG NEG
Cyclin D1 Status

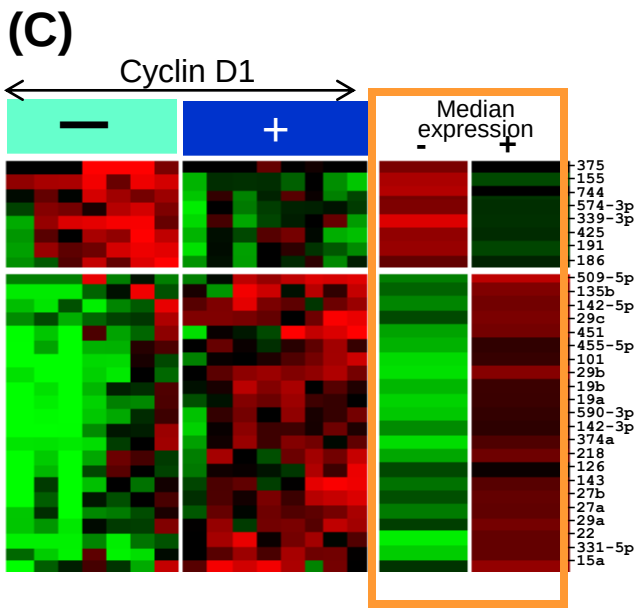
(C)
Cyclin D1
−
+
Median
expression
-
+
375
155
744
574-3p
339-3p
425
191
186
509-5p
135b
142-5p
29c
451
455-5p
101
29b
19b
19a
590-3p
142-3p
374a
218
126
143
27b
27a
29a
22
331-5p
15a

Figure 6

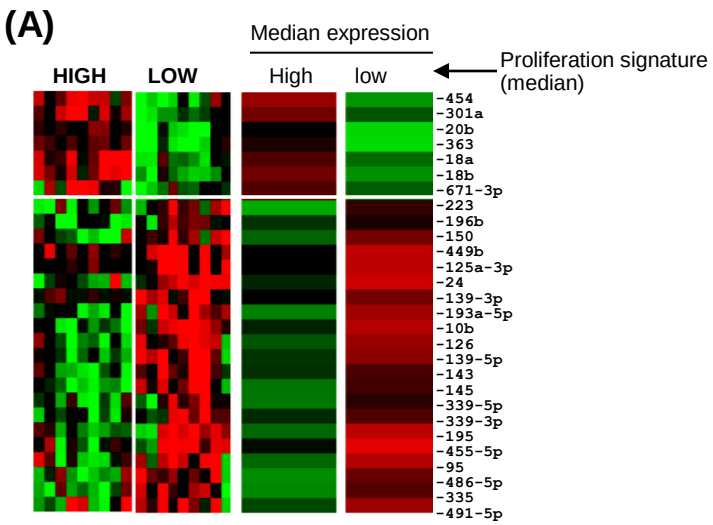
(A)
Median expression
HIGH
LOW
High
low
Proliferation signature (median)
-454
-301a
-20b
-363
-18a
-18b
-671-3p
-223
-196b
-150
-449b
-125a-3p
-24
-139-3p
-193a-5p
-10b
-126
-139-5p
-143
-145
-339-5p
-339-3p
-195
-455-5p
-95
-486-5p
-335
-491-5p

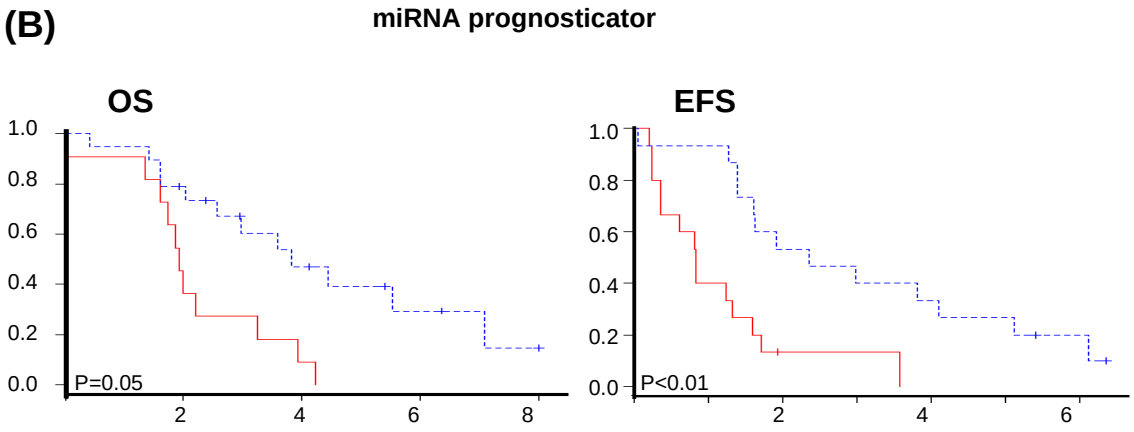
(B)
miRNA prognosticator
OS
EFS
1.0
0.8
0.6
0.4
0.2
0.0
P=0.05
P<0.01
2
4
6
8